

TUTORIAL ON DIRECT DIGITAL SYNTHESIZER STRUCTURE IMPROVEMENTS AND
STATIC TIMING ANALYSIS

BY

ZEXIAN LI

THESIS

Submitted in partial fulfillment of the requirements
for the degree of Master of Science in Electrical and Computer Engineering
in the Graduate College of the
University of Illinois at Urbana-Champaign, 2018

Urbana, Illinois

Adviser:

Professor Jose E. Schutt-Aine

ABSTRACT

The direct digital frequency synthesizer (DDS) has been widely used in digital communication systems due to its high frequency resolution, fast frequency conversion, and continuous phase change. With the development of microelectronics technology, field-programmable gate array (FPGA) devices have been rapidly developed. Because of FPGAs' high speed, high integration and field-programmable advantages, the devices are widely used in digital processing and are increasingly favored by hardware circuit design engineers. FPGAs also provide a technique for using digital data processing blocks as a means to generate a frequency and phase tunable output signal referenced to a fixed-frequency precision clock source. Many telecommunication applications require such high-speed switching, fine tunability and superior quality signal source for their components. This thesis will introduce the direct digital synthesizer (DDS) and investigate some ways to optimize the DDS structure to save hardware resources and increase chip speed without sacrificing signal quality.

The Verilog hardware description language is used as the development language. This thesis will describe entire designs of both DDS with traditional structure and DDS with new structures. By comparing the outputs, it also examines the corresponding simulation results and verifies the improvement of the signal quality.

To my family, for their love, support, motivation and patience.

To my adviser, for his support, guidance and advice.

To my student coworkers, for their advice and help.

ACKNOWLEDGMENTS

I would like to thank my graduate school adviser, Professor Jose E. Schutt-Aine, for all his kind help, support, encouragement and guidance along the way. He is a very kind and knowledgeable professor who is always willing to help the students when they are in need. I have greatly benefited from Professor Schutt-Aine's profound knowledge, rigorous academic attitude, practical work style and spirit of seeking truth and knowledge. I feel very blessed that I have had the opportunity to learn from and work with my brilliant adviser and his research group in these past years. And thanks to the visiting scholar Lan Chen who helped me during her visiting time and gave me some perspectives I had not thought of before.

Also, I would like to give my special thanks to my good friends and colleagues: Xinying Wang, Xu Chen, Xiao Ma, Nancy Zhao, Ashwarya Rajwardan, Bobi Shi, Thong Nguyen, Pin-Chiao Huang and Bohao Wu for the invaluable discussions, all the late nights and indelible memories we have together.

Last but not least, I would like to give my sincere thanks to my parents for all their support, patience, understanding and love.

TABLE OF CONTENTS

CHAPTER 1: INTRODUCTION.....	1
1.1 Purpose and Motivation.....	1
1.2 Outline	3
CHAPTER 2: TRADITIONAL AND NEW STRUCTURE DDS FUNDAMENTALS.....	4
2.1 Basic Working Principle of Traditional DDS.....	4
2.2 Basic Working Principle of New Structure of DDS.....	9
CHAPTER 3: FPGA DESIGN FLOW AND DESCRIPTION.....	15
CHAPTER 4: DDS FPGA DESIGN AND SIMULATION RESULTS.....	19
CHAPTER 5: DDS TIMING REPORTS AND STATIC TIMING ANALYSIS TUTORIAL....	24
5.1 Static Timing Analysis.....	24
5.2 Static Timing Analysis for FPGA.....	24
5.3 Factors Limiting the Maximum Frequency of the FPGA.....	25
5.4 TimeQuest Basic Process.....	26
CHAPTER 6: SPURS IN THE DDS.....	33
CHAPTER 7: CONCLUSION AND FUTURE WORK.....	37
REFERENCES	38

CHAPTER 1: INTRODUCTION

1.1 Purpose and Motivation

The direct digital synthesizer (DDS) is a popular technique for frequency synthesis. The main idea of DDS is using digital data processing blocks as a means to generate a frequency- and phase-tunable output signal referenced to a fixed-frequency precision clock source. Today's cost-competitive, high-performance, functionally integrated, and small package-sized DDS products are fast becoming an alternative to traditional frequency-agile analog synthesizer solutions [1]. The topology of a conventional direct digital synthesizer (DDS) is shown in Figure 1.1 which consists of five primary elements: a driving clock, a phase accumulator (PA), a look-up table (LUT), a digital-to-analog converter (DAC), and a reconstruction filter [2]. It was presented by Tierney, Rader and Gold in 1971 [3]. The traditional DDS will be explained and discussed in more detail in Chapter 2. [2]

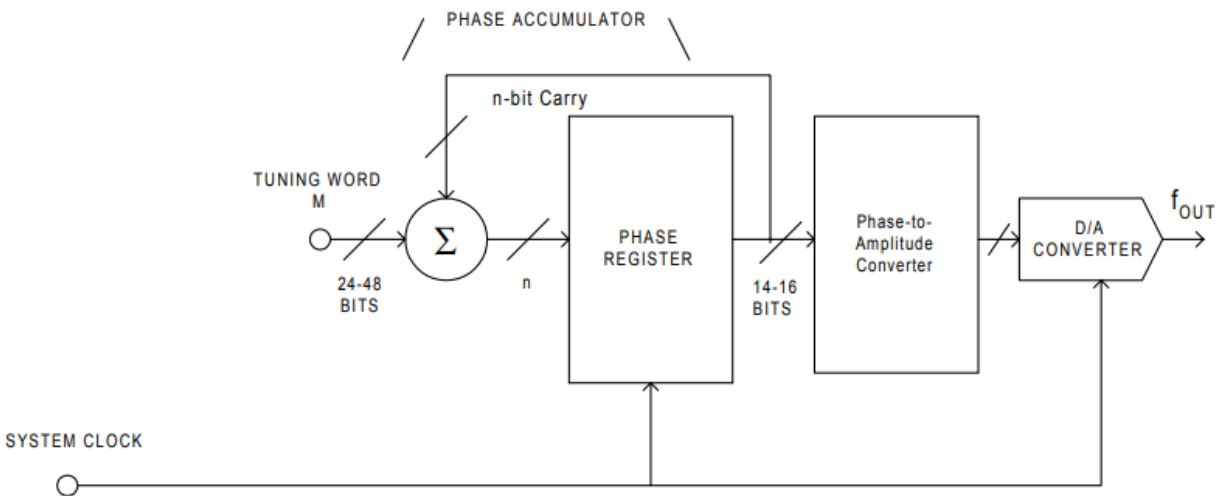


Figure 1.1: Basic structure of a generic direct digital synthesizer

The PLL offers very good wide tuning bandwidth due to the use of a programmable divider as compared to DDFS approach [4]. On the other hand, DDFS provides many significant advantages such as fast settling time, sub-hertz frequency resolution, continuous-phase switching response

and low phase noise [5], [6]. Compared with other frequency synthesizing techniques such as VCO, DDS gives much higher frequency resolution, faster frequency channel switching with continuous phase, wider range of frequency tuning and more flexible and versatile modulation capability [7]. Nowadays, the cost-competitive, high-performance, functionality-integrated and small-package DDS products are widely used in the field of telecommunications and are becoming an alternative to some traditional analog synthesizer solutions. The applications of DDS include signal generation, local oscillators, function generators, mixers, modulators, and sound synthesizers. The advantages of DDS are the following: (1) DDS has micro-hertz tuning resolution of the output frequency and sub-degree phase tuning capability, all under complete digital control. (2) DDS has extremely fast “hopping speed” in tuning output frequency (or phase), phase-continuous frequency hops with no over/undershoot or analog-related loop settling time anomalies. (3) The DDS digital architecture eliminates the need for the manual system tuning and tweaking associated with component aging and temperature drift in analog synthesizer solutions. (4) The digital control interface of the DDS architecture facilitates an environment where systems can be remotely controlled, and minutely optimized, under processor control. (5) When utilized as a quadrature synthesizer, DDS affords unparalleled matching and control of I and Q synthesized outputs [8].

This thesis uses an optimized design of DDS to minimize hardware complexity, reduce chip area and power consumption, and increase chip speed while maintaining the original advantages of DDS. The DDS will be designed and implemented in Verilog codes that are synthesizable on an FPGA. FPGA is widely used in digital circuit design for its flexibility, accuracy and effectiveness.

The most significant advantage of using an FPGA is that designs can be created and changed in a very short period. Instead, with application-specific integrated circuits (ASICs), the designers will have to wait months for the circuits to be fabricated.

1.2 Outline

This thesis will serve as a complete tutorial on the background knowledge of DDS with the traditional structure and DDS with the new structure to save resources without sacrificing the performance.

- Chapter 2 provides an overview of the theory and structure of the DDS with both traditional and new structure.
- Chapter 3 introduces the background knowledge of FPGA and the FPGA design flow.
- Chapter 4 presents the implementation and simulation difference between traditional DDS and DDS with new structure on FPGA in Altera Quartus FPGA development software.
- Chapter 5 presents the simulation results from the different structures of DDS and some theoretical analysis of the results. This chapter will focus on the optimized design of DDS which is to minimize hardware complexity, reduce chip area and power consumption, and increase chip speed while maintaining the original advantages of DDS.
- Chapter 6 concludes this thesis with a summary and potential research topics and improvements.

CHAPTER 2: TRADITIONAL AND NEW STRUCTURE DDS FUNDAMENTALS

2.1 Basic Working Principle of Traditional DDS

A traditional DDS is composed of four components: a phase accumulator (PA) which includes a register, a lookup table (LUT), a digital-to-analog converter (DAC) and a low-pass filter (LPF) as shown in Figure 2.1.

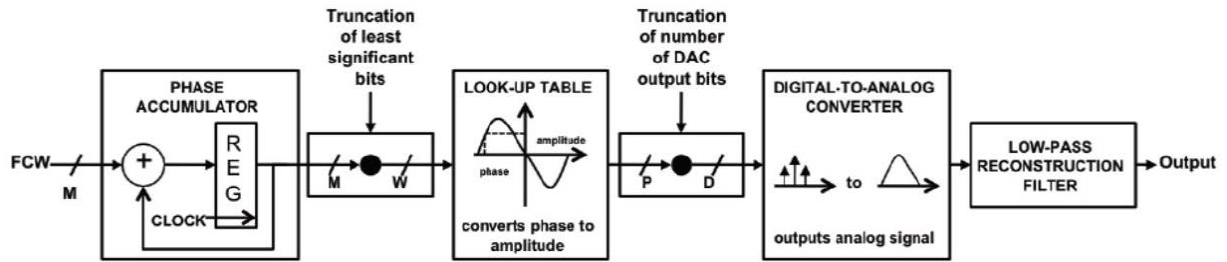


Figure 2.1: Basic structure of traditional DDS

The circuit starts with a frequency control/tuning word (FCW/FTW) applied to the PA. At each clock cycle, the PA keeps incrementing by the M-bit FTW ($M=32$ for this design) and the result is stored in an inbuilt register. The output of this register is fed back and added to the input FTW creating a cycle. The output of the PA is then truncated and given to the LUT. The process of truncation is a simple elimination of the lower order bits. The LUT then accepts the W-bit word as the phase of the sine wave and in turn generates the amplitude of a sine wave. Hence the LUT is also called a phase-to-amplitude converter. This quantized version of the sine wave is then fed into the DAC which creates an analog output. The LPF at the end smoothens the output of the desired signal [9].

Figure 2.2 shows the block diagram for direct digital synthesis-based waveform generation.

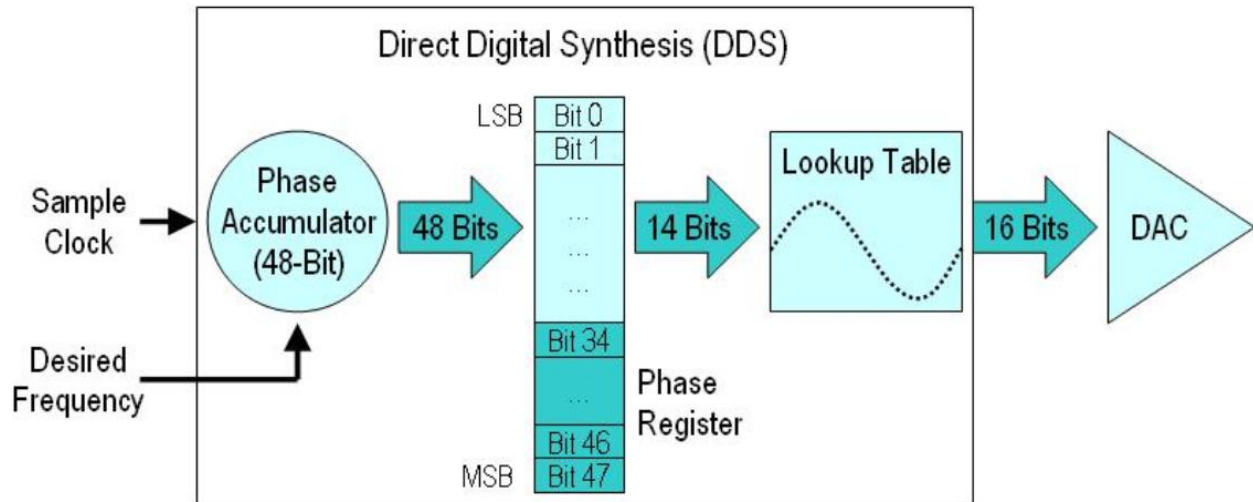


Figure 2.2: Direct digital synthesis block diagram

Phase Accumulator (PA): The PA is principally a combination of an adder, a counter and a register. At each clock cycle the M-bit word of the PA increments by the FTW, thereby producing a quantized saw-tooth waveform as in Figure 2.3 [2]. Each dot on the saw-tooth waveform is the value that comes out of the register.

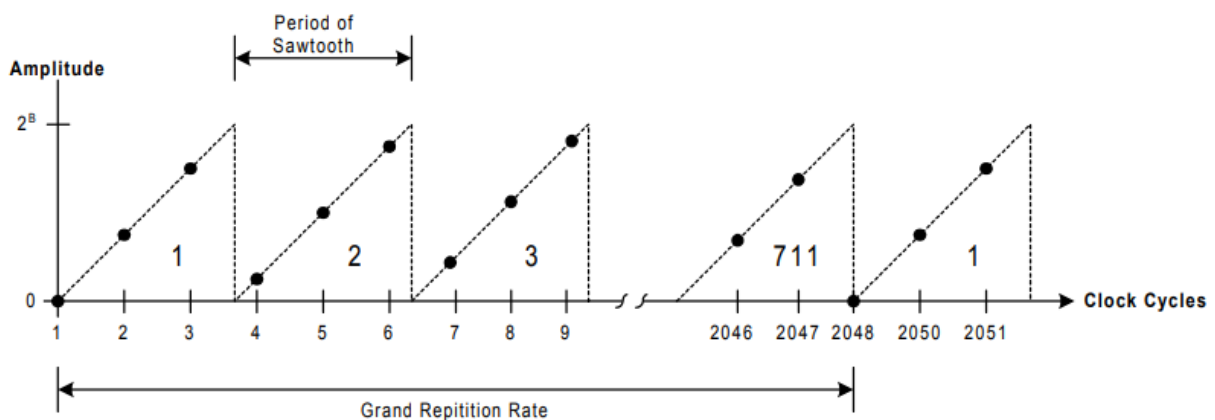


Figure 2.3: Saw-tooth output of phase accumulator

Now since we give an input of an M-bit word, the PA has 2^M possible values. The final frequency of the sine wave is directly dependent on the frequency of this saw-tooth waveform produced at

the PA. Thus, the larger the M word, the faster the PA jumps, which leads to a higher frequency at the output. From the output of the PA we could derive the ultimate frequency of the sine wave as in Equation 2.1:

$$f_{out} = F_{TW}/2^M * f_{clk} \quad (2.1)$$

And because DDS follows Nyquist's sampling law, the highest output frequency is half the clock frequency. In practice, the highest output frequency of the DDS is determined by the spur level of the allowable output, which is generally $f_o \leq 40\% f_c$.

As Figure 2.2 illustrates, a phase accumulator compares the sample clock and desired frequency to increment a phase register. Again, the fundamental idea is that we can generate signals with precise frequencies by generating an appropriate sample based on the phase of that frequency at any point in time. In addition, by representing our waveform with 2^{14} (16,384) points, we are able to represent exactly 16,384 phase increments with our lookup table. The phase accumulator uses simple arithmetic operations to calculate the lookup table address for each generated sample. It does this by dividing the desired frequency by the sample clock and multiplying the result by 2^{48} . This number is based on the bit resolution of the phase register. For NI signal generators, a 48-bit phase register is used for maximum precision. Of these, 34 bits are used to store the remainder phase, and 14 bits are used to choose a sample from the lookup table.

Thus, the phase accumulator produces a 14-bit address that corresponds to the exact phase of the signal. For example, an address of '00000000000000' corresponds to 0° . On the other hand, an address of '11111111111111' corresponds to 359.978° . Thus, the signal generator can use this address to control the phase of the signal at any point in time. This process is shown in Figure 2.4.

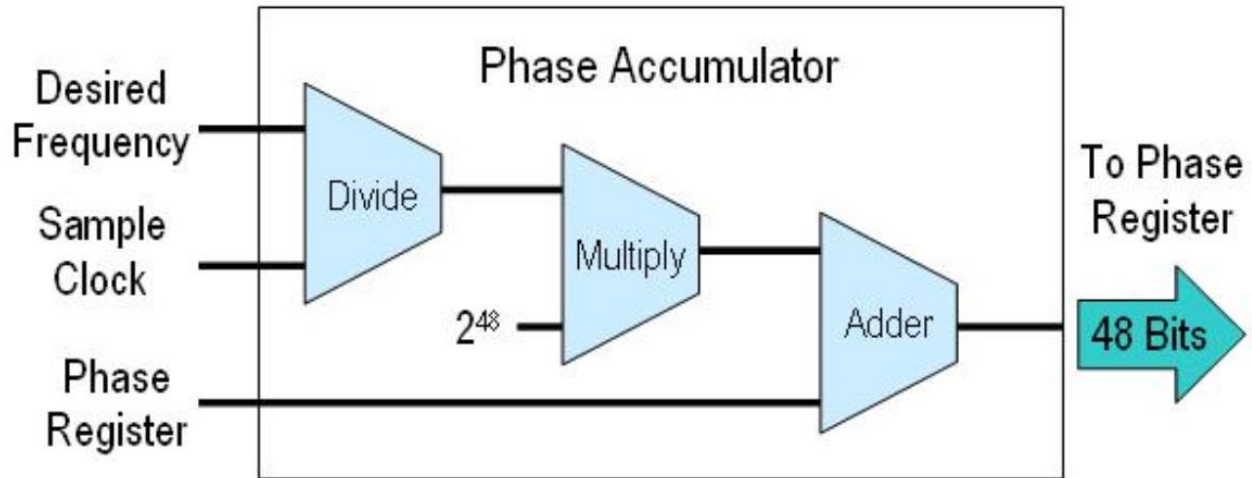


Figure 2.4: Computation of the phase register

As Figure 2.4 suggests, the phase accumulator is able to represent the phase of the generated signal with 2^{48} points of precision. However, because we only have 2^{14} available points in our waveform, only the 14 most significant bits of the phase register are used in the lookup table. The remaining 34 bits are used to store the remainder of the phase increment. This remainder enables the DDS precision by ensuring that the lookup table will return the appropriate phase information after the phase register rolls over (once per period of the waveform) [8].

Lookup Table (LUT): The LUT behaves as a phase-to-amplitude conversion unit, thereby giving us a discrete sine wave at the output. To keep the LUT reasonably sized we truncate the bits from the PA and feed the higher order bits to the LUT [10]. For our design we choose bits 29 through 18 as the 12 bit W-word. This allows the hardware to be reasonably sized and not extremely power hungry. The LUT will contain unique values of a sine wave over one period; however even in that one period, the sine wave is symmetrical. To further exploit this symmetrical nature, we can fill the table with values that correspond to only a quarter of a sine wave period [10].

For the FPGA design, one will need a coefficients file containing the values of the LUT. Generate this file with the help of Matlab and store it as a '*.coe'. This file will then be added to the ROM.

Digital-to-Analog Converter (DAC): A second truncation process is carried out here, as the output of the LUT is truncated to the appropriate number of bits and then given to the DAC. The DAC creates an analog waveform from the discretized sine wave. An important fact to note here is that the DAC is solely responsible for limiting the design's maximum attainable frequency. It does not matter how fast the PA is clocked as the DAC (which is one of two analog components in the entire design) forms the bottleneck.

Low-Pass Filter (LPF): The LPF behaves as a reconstruction filter that smoothens the signal from the DAC. Since we do not want any aliases of the fundamental frequency, this LPF also behaves as an antialiasing filter [3], thereby limiting us to the Nyquist frequency. Typically, a Chebyshev filter is used to build this stage due to its sharp frequency response characteristics [3].

In summary, the traditional DDS structure can be simplified as shown in Figure 2.5.

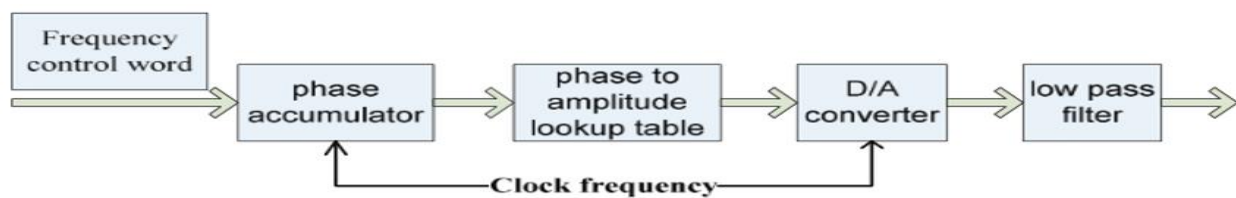


Figure 2.5: Traditional DDS structure block diagram

And the traditional DDS structure Quartus generated block diagram is as shown in Figure 2.6.

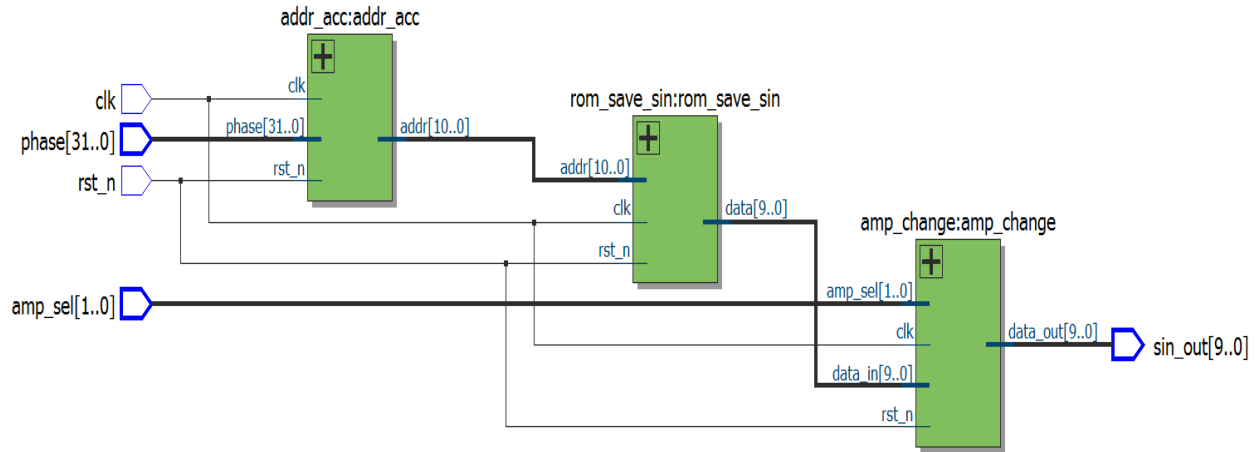


Figure 2.6: Traditional DDS Quartus generated block diagram

2.2 Basic Working Principle of New Structure of DDS

Similar to the traditional DDS structure, the new structure DDS block diagram is in Figure 2.7.

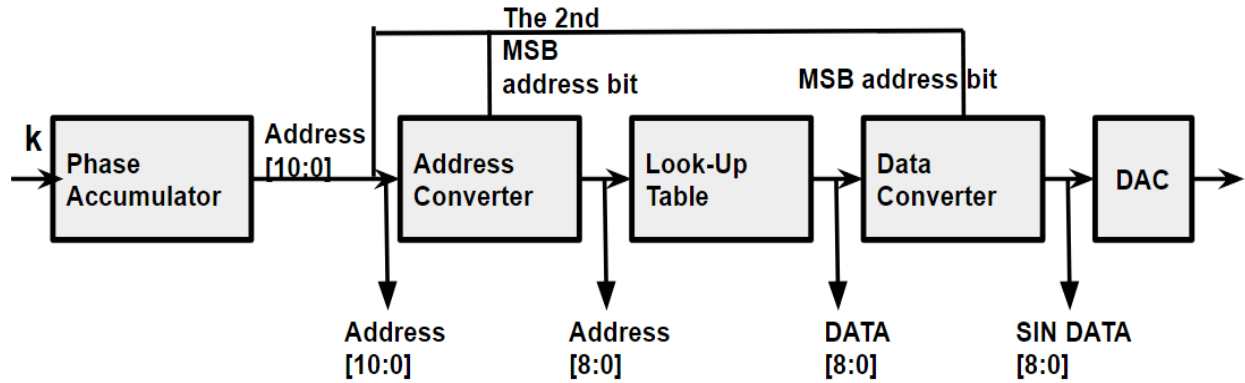


Figure 2.7: New structure DDS block diagram

The new DDS's address converter is based on the value of the 2nd most significant address bit to determine whether the value is increasing from cycle 0 to $\pi / 2$ or decreasing from cycle $\pi / 2$ to π , while the data converter is based on the most significant address bit to determine whether the first half of the generated waveform is from cycle 0 to π or the second half-cycle from π to 2π .

Based on the above theory, the sine address change converter block module is shown below in Figure 2.8:

```

1  module sin_addr_change(
2      input [10:0] iaddr,
3      output reg [8:0] oaddr
4  );
5
6      always@(*)
7          if(iaddr[9])
8              oaddr <= iaddr[8:0] ^ 9'h1fff;
9          else
10             oaddr <= iaddr[8:0];
11
12 endmodule

```

Figure 2.8: Sine address change module codes

And the data change converter block Verilog code is provided in Figure 2.9.

```

1  module data_change(
2      input clk,
3      input rst_n,
4      input [10:0] iaddr,
5      input signed [8:0] data_in,
6      output reg signed [9:0] data_out
7  );
8
9      reg [10:0] iaddr_d1;
10
11     always@(posedge clk or negedge rst_n)
12         if(!rst_n)
13             iaddr_d1 <= 11'd0;
14         else
15             iaddr_d1 <= iaddr;
16
17     always@(*)
18         if(iaddr_d1[10])
19             data_out <= 10'd0 - data_in;
20         else
21             data_out <= {1'b0, data_in};
22
23 endmodule

```

Figure 2.9 Data change module codes

The new DDS structure employs four pipelines. The 32-bit accumulator is divided into four pipelines, each pipeline completing the 8-bit addition operation, and the pipeline's carry is cascaded. The pipeline structure can improve the accumulator operation speed by more than three times. In order to improve the operation speed, the adder uses the fastest carry-lookahead bit algorithm. The pipeline structure can improve the operation speed of the device. However, the

disadvantage is that the data needs to be kept for four clock cycles, which reduces the frequency of the system hopping. The main codes of the four carry-forward adders are shown in Figure 2.10 and Figure 2.11. And the block diagram for the four-pipelining structure is shown in Figure 2.12.

```

13
14  wire [8:0] temp1;
15
16  assign temp1 = add_addr0 + phase[7:0];
17
18  always@(posedge clk or negedge rst_n)
19      if(!rst_n)
20          add_addr0 <= 8'd0;
21      else
22          add_addr0 <= temp1;
23
24
25  wire [8:0] temp2;
26
27  assign temp2 = add_addr1 + phase[15:8];
28
29  always@(posedge clk or negedge rst_n)
30      if(!rst_n)
31          add_addr1 <= 8'd0;
32      else
33          add_addr1 <= temp2 + temp1[8];
34
35
36  wire [8:0] temp3;
37
38  assign temp3 = add_addr2 + phase[23:16];
39

```

Figure 2.10: Four carry-lookahead adders codes partI

```

40  always@(posedge clk or negedge rst_n)
41      if(!rst_n)
42          add_addr2 <= 8'd0;
43      else
44          add_addr2 <= temp3+ temp2[8];
45
46
47  always@(posedge clk or negedge rst_n)
48      if(!rst_n)
49          add_addr3 <= 8'd0;
50      else
51          add_addr3 <= add_addr3 + phase[31:24]+ temp3[8];
52
53
54  wire [31:0] out_addr;
55
56  assign out_addr = {add_addr3,add_addr2,add_addr1,add_addr0};
57
58  assign addr = out_addr[31:21];
59

```

Figure 2.11: Four carry-lookahead adders codes partII

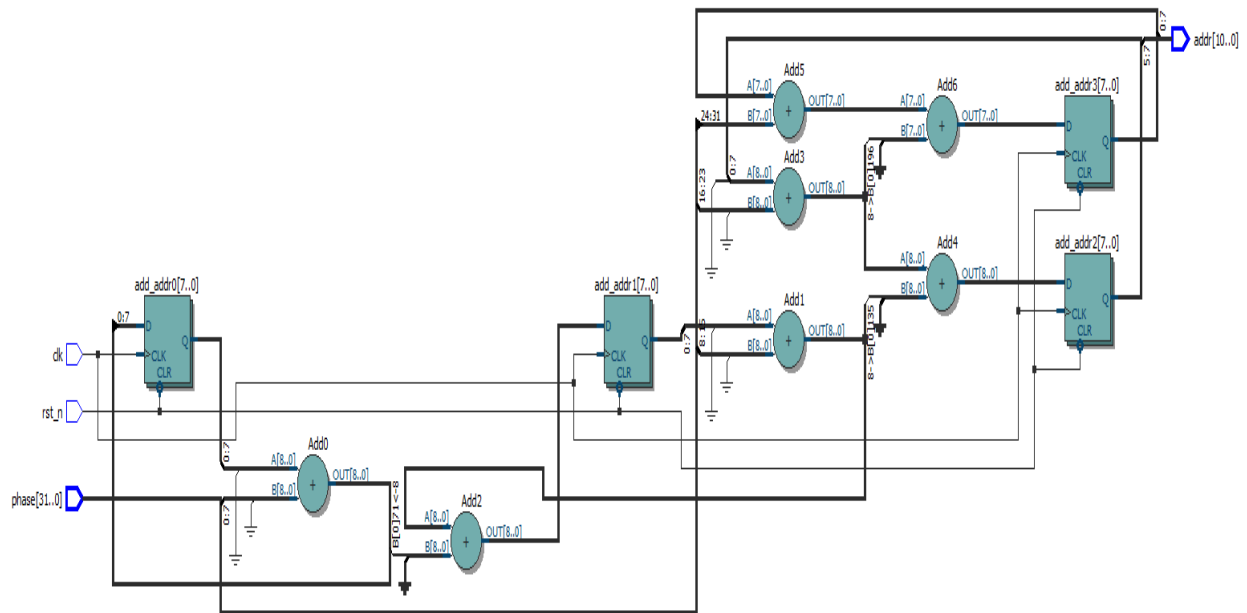


Figure 2.12: Four pipeline structure block diagram

And after simulation, Figure 2.13 and 2.14 below show that with the new pipeline structure, the maximum operating frequency rises from 284.82 MHz to 307.22 MHz, which is consistent with the goal of the design. And the maximum allowed frequency (Fmax) can be found under the TimeQuest Timing Analyzer -> Fmax Summary. The TimeQuest Timing Analyzer is used for timing analysis in Quartus II which will be explained in more detail in Chapter 5.

Slow 1200mV 85C Model Fmax Summary				
	Fmax	Restricted Fmax	Clock Name	Note
1	284.82 MHz	250.0 MHz	clk	limit due to minimum period restriction (max I/O toggle rate)

Figure 2.13: Maximum operating frequency of traditional DDS

Slow 1200mV 85C Model Fmax Summary				
	Fmax	Restricted Fmax	Clock Name	Note
1	307.22 MHz	250.0 MHz	clk	limit due to minimum period restriction (max I/O toggle rate)

Figure 2.14: Maximum operating frequency of new structure DDS

For the compression of the ROM table, the second highest bit of the phase accumulator is used to determine the quadrant, and the sinusoidal composite wave is synthesized into the range of 0 to π ; the highest bit is used as the sign bit, and the sine wave is synthesized into the range of 0 to 2π . For a cosine wave, the sign bit is obtained by XORing the highest bit and the next highest bit because the cosine waveform is $\pi/2$ phase ahead of the sinusoidal waveform. But since the sine function and the cosine function are symmetric about $\pi/4$, it is possible to store only the sine and cosine function values of (0 to $\pi/4$), so that the memory size will be reduced by half. The second highest bit of the phase accumulator can be selected between 0 to $\pi/4$ and $\pi/4$ to $\pi/2$. When the actual circuit is implemented, the next high bit is XORed with the next highest bit to generate this signal. In addition, in order to complete the quadrature output, two 2:1 multiplexer circuits are added.

Last but not the least, the last block change is the amplitude change module which saves more resources to select to output the corresponding amplitude. The Verilog code for the amplitude change module is provided in Figure 2.15.

```

1  module amp_change(
2      input clk,
3      input rst_n,
4      input [1:0]amp_sel,
5      input [9:0] data_in,
6      output reg [9:0] data_out
7  );
8
9  always@(posedge clk or negedge rst_n)
10     if(!rst_n)
11         data_out <= 10'd0;
12     else if(amp_sel == 2'd0)
13         data_out <= data_in;
14     else if(amp_sel == 2'd1)
15         data_out <= {data_in[9],data_in[9:1]};
16     else if(amp_sel == 2'd2)
17         data_out <= {data_in[9],data_in[9],data_in[9:2]};
18     else if(amp_sel == 2'd3)
19         data_out <= {data_in[9],data_in[9],data_in[9], data_in[9:3]};
20
21 endmodule

```

Figure 2.15: Amplitude change module codes

The new DDS structure Quartus generated block diagram is shown in Figure 2.16.

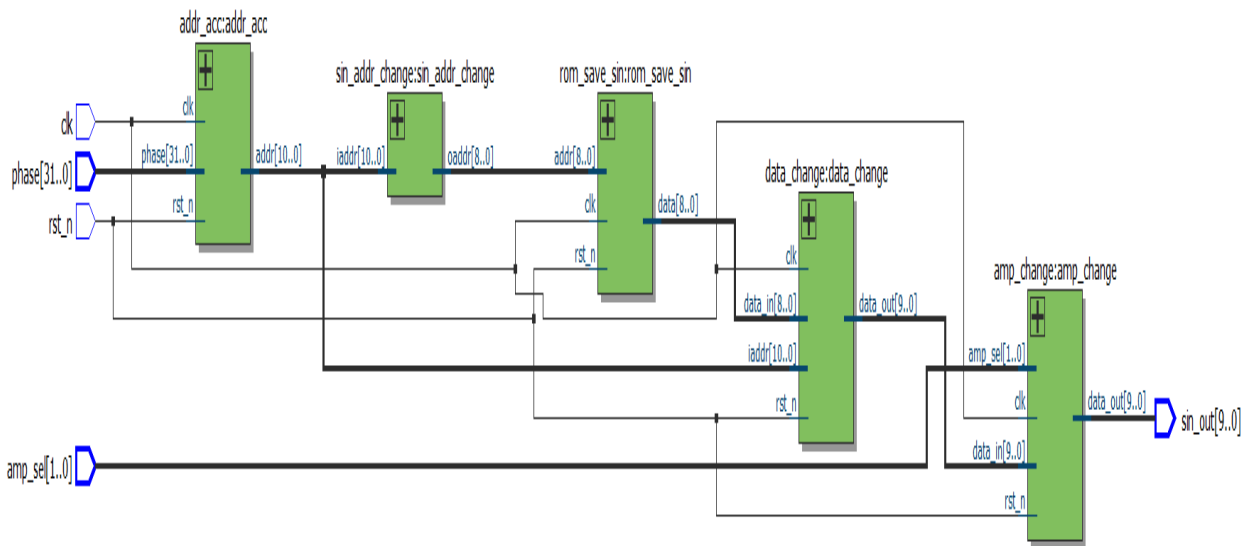


Figure 2.16: New structure DDS Quartus generated block diagram

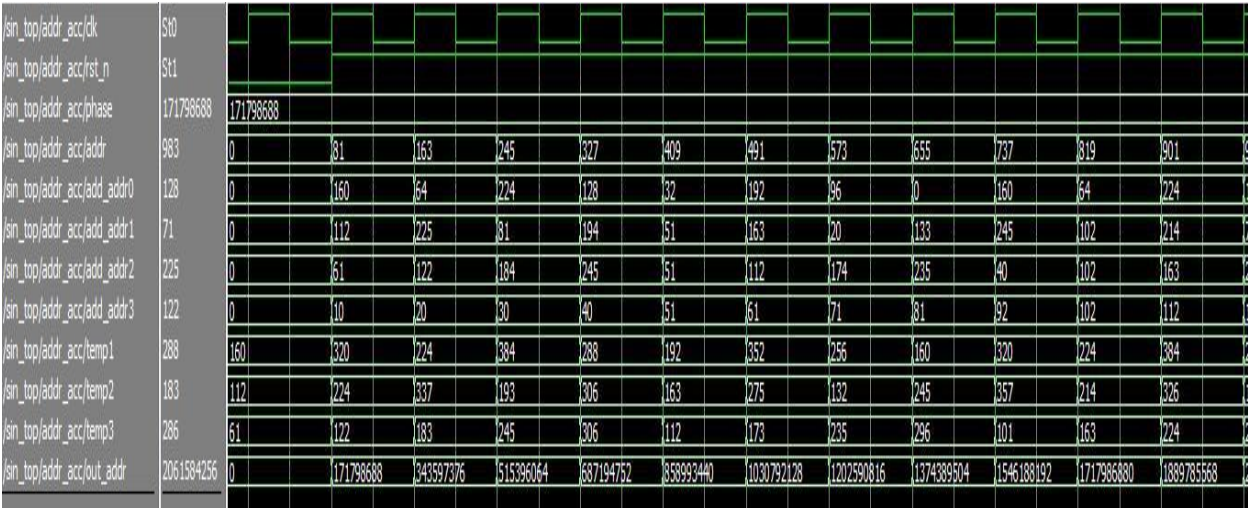


Figure 2.17: New structure DDS signals waveform

Figure 2.17 shows the intermediate signals in the new structure DDS design implementation. Based on these new improvements analysis, the new DDS's resource usages should be saved as compared to the traditional DDS structure. More simulation results and comparisons will be shown in the later chapters.

CHAPTER 3: FPGA DESIGN FLOW AND DESCRIPTION

There are two typical ways to design and implement digital circuits: application-specific integrated circuits (ASIC) implementation and field-programmable gate array (FPGA) implementation. The main difference between the two is that in the case of the FPGAs one can program a ready development board and thus implement and test the design setup more quickly. ASICs, however, are capable of a complete custom design, which makes them cheaper and smaller since the device only contains components that are absolutely necessary to run the application. More comparisons are listed in Figure 3.1. From a research standpoint it is recommended to use an FPGA since one can easily modify designs and test them using the numerous test switches and ports that are present on board. Hence for this project a DDS will be implemented on an FPGA.

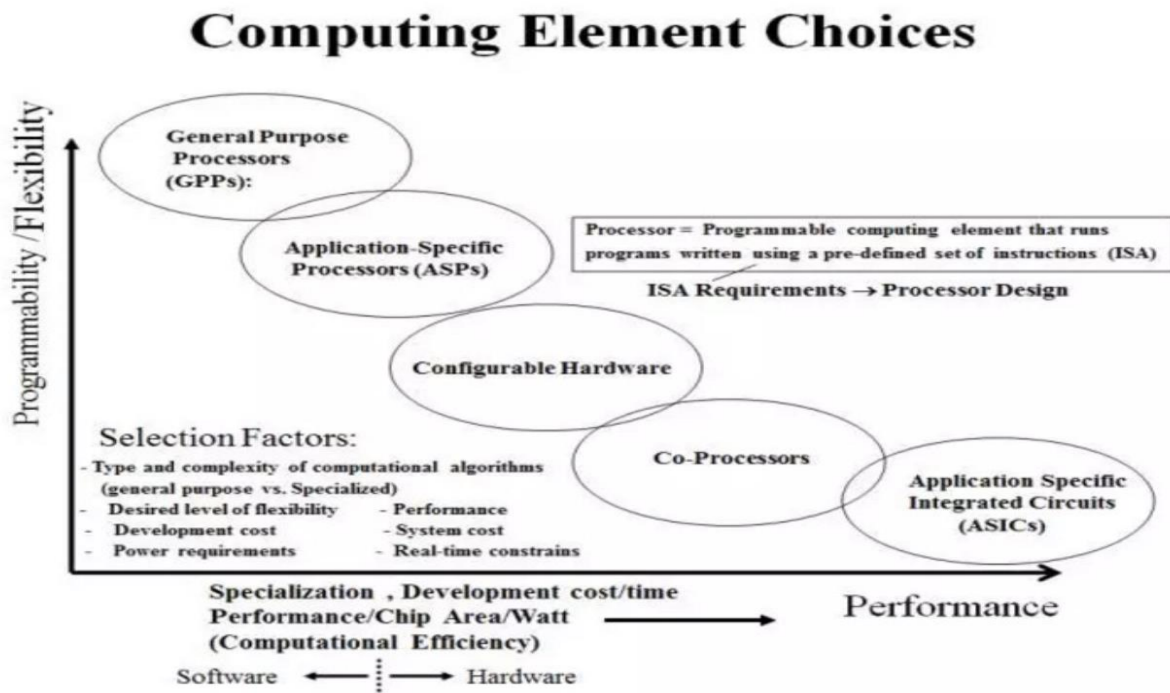


Figure 3.1: Computing element choices pros and cons comparisons

Shown in Figure 3.2 is a rough FPGA process design flow that every person should follow when designing a circuit [11]. Note that Design Entry includes Functional/Device Specification and HDL Coding, and Implementation includes Mapping and Placement and Route.

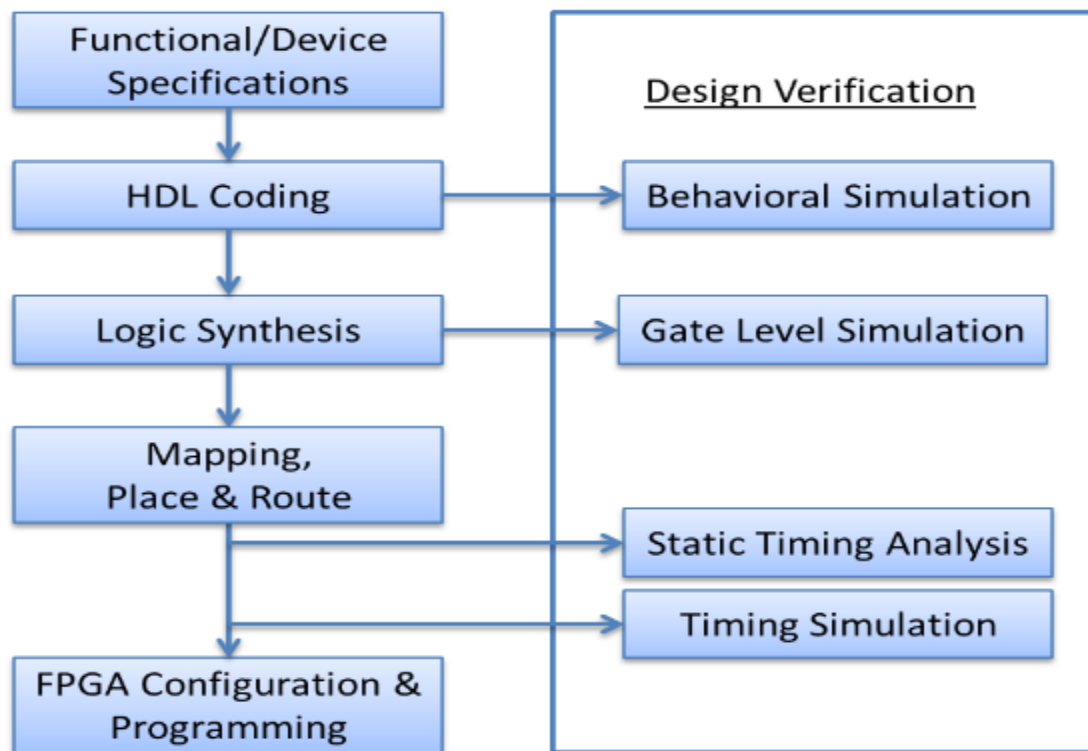


Figure 3.2: FPGA design flow block diagram

Functional/Device Specifications: In this stage, the designer sets up the configuration (make/model/speed/class/device family) of the FPGA. After that, the design software will conduct some preliminary setup for the particular FPGA device's intellectual property (IP), designs and components [12], [13].

Hardware Description Language (HDL) Coding: For this step, the designer codes the entire design into a hardware-readable language (Verilog or VHDL). The designer also has the option to

implement the project via a schematic based entry; however, when one needs to utilize algorithms for the design, an HDL-based entry is preferred [12], [13].

Logic Synthesis: Synthesis is a process that converts the HDL codes to the gate-level netlist, which describes the different types of components, elements, and interconnections between the components and other details like area occupied and temperature of operation, etc. Also, synthesis will help check the syntax of the HDL codes and map the design to a particular FPGA family [12], [13].

Mapping: This process maps the generic logic design (which is composed of different gates, flip flops, modules and inputs/output switches) to the logic technology contained in the selected FPGA device [12], [13].

Placement and Route (PAR): This stage is one of the most important steps in the entire implementation. Placement decides where the components should be placed on the FPGA while routing is responsible for the connections between different components. PAR is crucial because it is related with the timing and area constraints of the design. A bad placement will result in problematic routing, which leads to design violations [14].

FPGA Configuration and Programming: The last step of the FPGA design flow is to program the designs on the FPGA and test the circuit. In this stage, the software converts the entire design to a “bitstream” file, which is loaded on the FPGA board. After that, the FPGA is ready to run the digital design [14].

Design Verification: It is extremely important for every design to meet certain standards and satisfy certain conditions. After each design step, the designers need to check whether the circuits meet various constraints such as timing, area and functional logic. In this thesis, we will use ModelSim as the simulation tool for design verification. The descriptions of each testing stage are given below:

1. Behavioral Simulation: This task is to verify the functionality of the HDL codes.
2. Gate-Level Simulation: The gate-level netlist is generated after the completion of synthesis. This task is to test the timing and gate-level functionality of the design.
3. Static Timing Analysis (STA): Once the PnR is completed and the STA is carried out, the designer can analyze important aspects of the circuit like setup and hold times for the circuit, critical paths within the circuit and clock skew rates. The STA will examine every possible path in the circuit and help debugging glitches and slow paths.
4. Post-PAR Timing Simulation: This is the final timing simulation after PnR. This simulation gives the designer an entire timing summary of the circuit, which is very close to the actual results seen when implemented on the FPGA [15].

Chapter 4: DDS FPGA DESIGN AND SIMULATION RESULTS

The traditional DDS device usage summary based on device Cyclone IV E EP4CE115F29C7 (the device used in ECE385 class) is shown in Figure 4.1.

Analysis & Synthesis Resource Usage Summary	
Resource	Usage
Estimated Total logic elements	62
Total combinational functions	61
Logic element usage by number of LUT inputs	
-- 4 input functions	17
-- 3 input functions	31
-- <=2 input functions	13
Logic elements by mode	
-- normal mode	30
-- arithmetic mode	31
Total registers	43
-- Dedicated logic registers	43
-- I/O registers	0
I/O pins	46
Total memory bits	20480
Embedded Multiplier 9-bit elements	0
Maximum fan-out node	clk~input
Maximum fan-out	53
Total fan-out	491
Average fan-out	2.38

Figure 4.1: Traditional DDS structure resource usage summary on device Cyclone
IV E: EP4CE115F29C7

The new structure DDS device utilization summary is shown in Figure 4.2.

Analysis & Synthesis Resource Usage Summary	
Resource	Usage
Estimated Total logic elements	96
Total combinational functions	94
Logic element usage by number of LUT inputs	
-- 4 input functions	17
-- 3 input functions	41
-- <=2 input functions	36
Logic elements by mode	
-- normal mode	40
-- arithmetic mode	54
Total registers	44
-- Dedicated logic registers	44
-- I/O registers	0
I/O pins	46
Total memory bits	4608
Embedded Multiplier 9-bit elements	0
Maximum fan-out node	clk~input
Maximum fan-out	53
Total fan-out	537
Average fan-out	2.25

Figure 4.2: New structure DDS structure resource usage summary on device Cyclone IV E: EP4CE115F29C7

The above device usage summary reports show that the new structure of DDS reduces the resource usage by three quarters from total memory bits 20480 to 4608.

Figures 4.3–4.6 show that the new structure DDS behavioral simulations are successful.

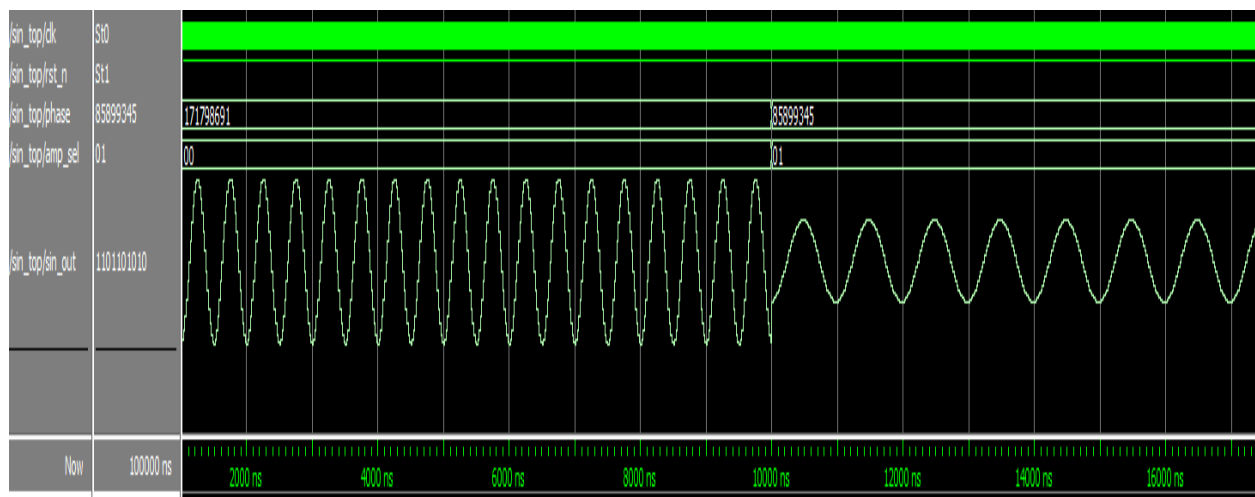


Figure 4.3: 32-bit 2MHz and 1MHz new structure DDS sine wave behavioral simulation

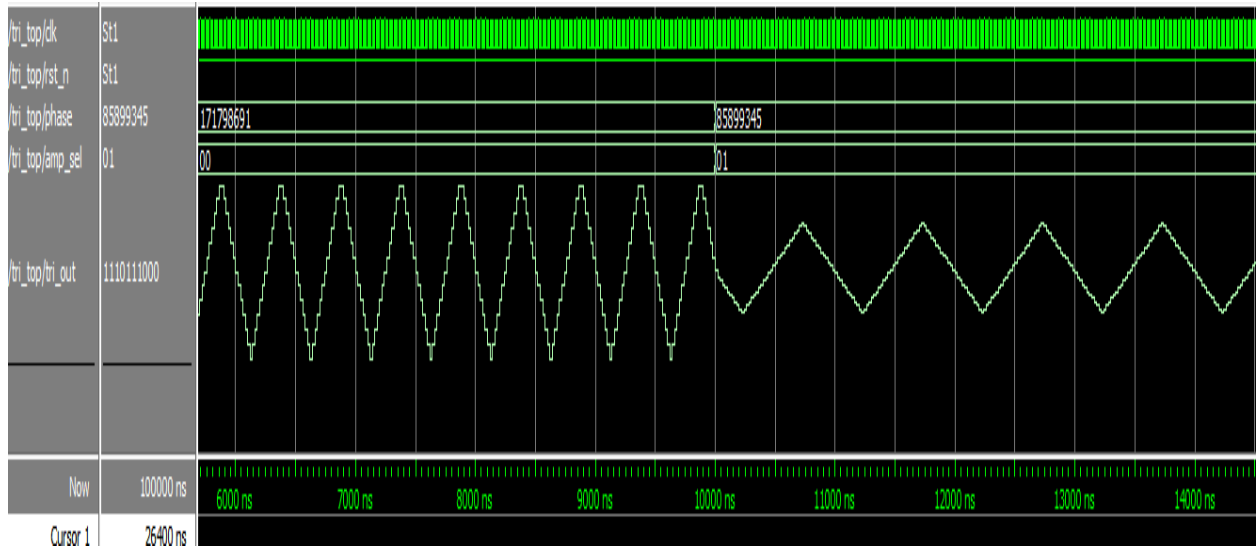


Figure 4.4: 32-bit 2MHz and 1MHz new structure DDS triangular wave behavioral simulation

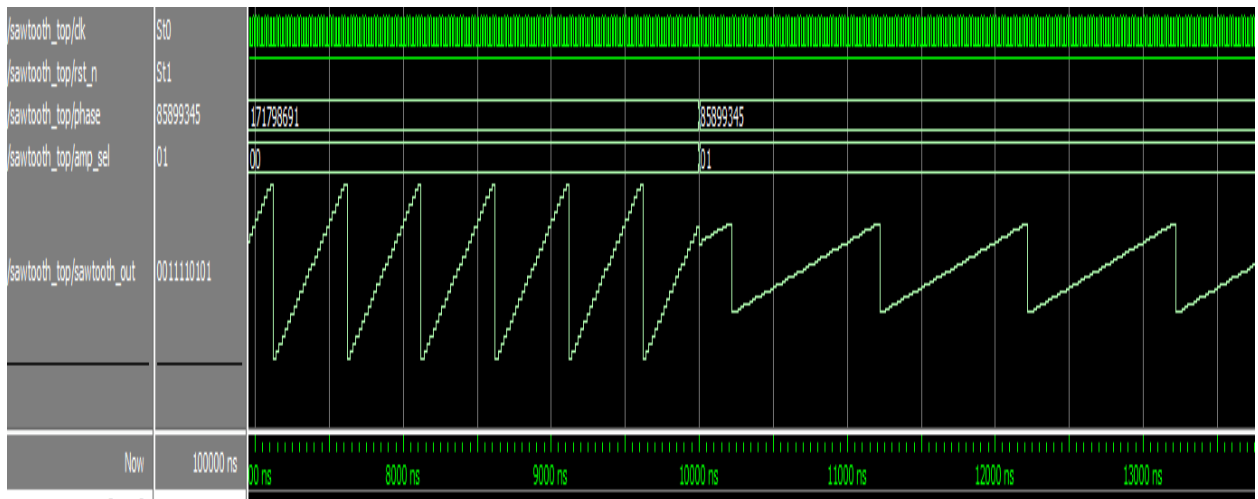


Figure 4.5: 32-bit 2MHz and 1MHz new structure DDS sawtooth wave behavioral simulation

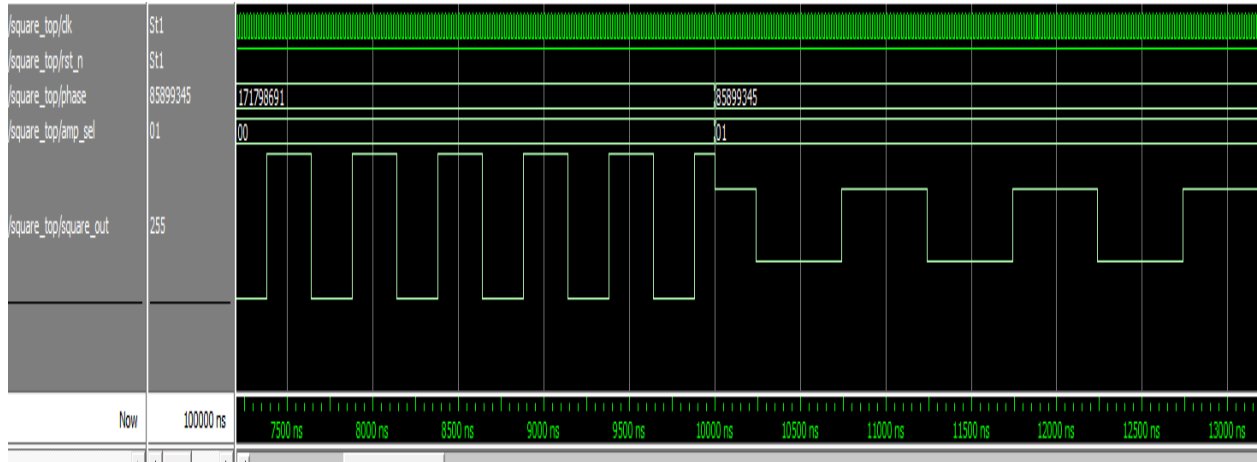


Figure 4.6: 32-bit 2MHz and 1MHz new structure DDS triangular wave behavioral simulation

Based on Figures 4.3–4.6, the proposed design is verified through the application of different input frequencies.

In Figures 4.3–4.6, given decimal number

85899345 (0b0000101000111101011100001010001)

and

171798691 (0b00001010001111010111000010100011)

as the FCW, we can calculate the output frequency to be 2MHz and 1MHz. From the distance in Figures 4.3–4.6, we can see that one full cycle of sine wave is 500ns and 1000ns, so the output frequency matches what we should have in theory. The 1MHz waveform's operating frequency amplitude is half of the 2MHz waveform's operating frequency, which could be selected by the amplitude select signal.

Figure 4.7 shows a summary of DDS waveforms in sine wave, triangular, sawtooth and square waveforms in two different frequencies and different amplitudes.

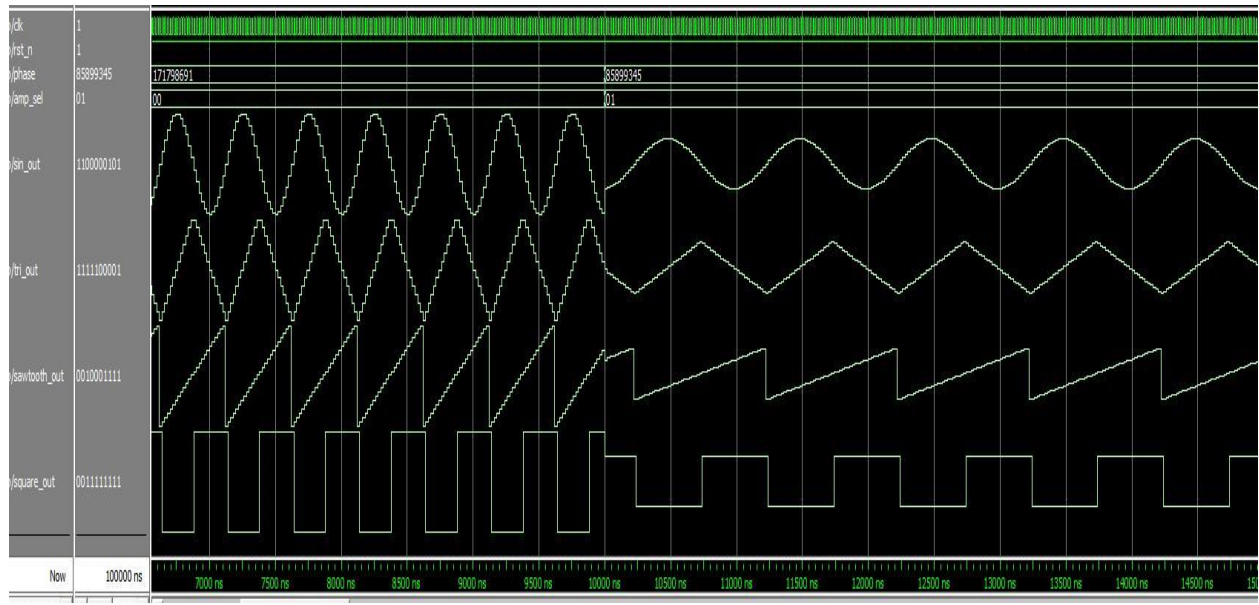


Figure 4.7: 32-bit 2MHz and 1MHz new structure DDS waves behavioral simulation summary

CHAPTER 5: DDS TIMING REPORTS AND STATIC TIMING ANALYSIS TUTORIAL

5.1 Static Timing Analysis

In static timing analysis, designers propose specific timing requirements (or add specific timing constraints), apply specific timing models, and analyze for specific circuits. The final result of the analysis is to require the system timing to meet the requirements set by the designer, that is, to achieve timing convergence.

5.2 Static Timing Analysis for FPGA

STA is applied to FPGA because the development tools do not know the requirements on our path. The designer tells the development tools the timing constraints and the tools re-plan according to the requirements to achieve the designer's timing requirements and to achieve timing closure.

After running the Implement Design process, Timing Analyzer could be used for a detailed analysis of the FPGA design. This ensures that the specified timing constraints were properly passed to the implementation tools. In addition, it is faster than timing-driven, gate-level simulation and helps design debugging. Performing a detailed analysis includes the following: (1) Verify that timing requirements were met for all paths in the design. (2) Analyze setup and hold performance for all constrained paths in the design. (3) Verify that operational frequencies are within component performance limits. (4) Analyze unconstrained paths to determine if any critical timing paths have been left unconstrained.

In a simple circuit, when the frequency is low, the edge time of the digital signal can be ignored, and there is no need to consider timing constraints. However, in complex circuits, in order to

reduce the delay of each part of the system, to make the system work together and improve the operating frequency, timing constraints are required. Usually, when the frequency is higher than 50 MHz, timing constraints need to be considered.

5.3 Factors Limiting the Maximum Frequency of the FPGA

Several factors limit the maximum frequency of the FPGA. The more the combination logic delays the gate circuit, the larger the combined logic delay. The FPGA actually uses the four-input look-up table (LUT, look-up-table) to implement the gate circuit, and the number of variables is less than four. All combinational logic delays are the same. When the number of variables is greater than four, multiple lookup table combinations are required, and the delay is increased. Signal path delay is the most important of all delays, and can even account for more than half of the total delay. Generally, EDA tools will not find the fastest path and need to apply timing constraints. The time that the clock is passed to each flip-flop will be offset by the length of the path from the clock source. The clock offset can be resolved by the structure of the H-tree. The clock jitter is caused by factors such as temperature distribution, signal crosstalk, etc., which cause the clock signals generated by the crystal oscillator, PLL, etc., to be not strictly equal. Additional constraints can be used to control the synthesis, mapping, placement, and routing of logic to reduce logic and routing delays, thereby increasing the operating frequency. In this thesis, path margin (slack) value will be analyzed, and based on this margin the FPGA synthesis, mapping, layout and routing will be optimized.

If there is a lot of combination logic in the design, then the signal will pass through multiple LUTs, which will also generate delay. In order to avoid the above problems, we need a high-speed

compiler as fast as the clock, and phase relationship and duty cycle. In this way, the compiler can calculate the delay according to our needs to compute the risk. All timing constraints are to tell the compiler what kind of relationship the clock and data should satisfy, and then hand it to the compiler to calculate the worst-case conditions that can be met, and how many will not satisfy the condition.

5.4 TimeQuest Basic Process

1). Precompile

As usual, first create a project, type the code as follows, assign the pin, and compile the project to get the gate-level netlist.

```
module dds
#( parameter PHASE_W = 24,
  parameter DATA_W = 16,
  parameter TABLE_AW = 12,
  parameter MEM_FILE = "SineTable.dat")
( input [PHASE_W - 1 : 0] FreqWord,
  input [PHASE_W - 1 : 0] PhaseShift,
  input Clock,
  input ClkEn,
  output signed [DATA_W - 1 : 0] Out
);
  reg signed [DATA_W - 1 : 0] sinTable[2 ** TABLE_AW - 1 : 0]; // Sine
  table ROM
  reg [PHASE_W - 1 : 0] phase; // Phase Accumulater
  wire [PHASE_W - 1 : 0] addr = phase + PhaseShift; // Phase Shift
```

```

    assign Out = sinTable[addr[PHASE_W - 1 : PHASE_W -
TABLE_AW]]; // Look up the table

```

```

initial begin

```

```

    phase = 0;

```

```

    $readmemh("SineTable.dat", sinTable); // Initialize the ROM

```

```

end

```

```

always@(posedge Clock) begin

```

```

    if(ClkEn)

```

```

        phase <= phase + FreqWord;

```

```

    end

```

```

endmodule

```

```

module dds_test(

```

```

    input CLOCK_50,

```

```

    output [15:0]GPIOO_D

```

```

);

```

```

    dds

```

```

    he_dds_inst(.FreqWord(24'h10000),.PhaseShift(24'h0),.Clock(CLOCK_5
0),.ClkEn(1'b1),.Out(GPIOO_D));

```

```

Endmodule

```

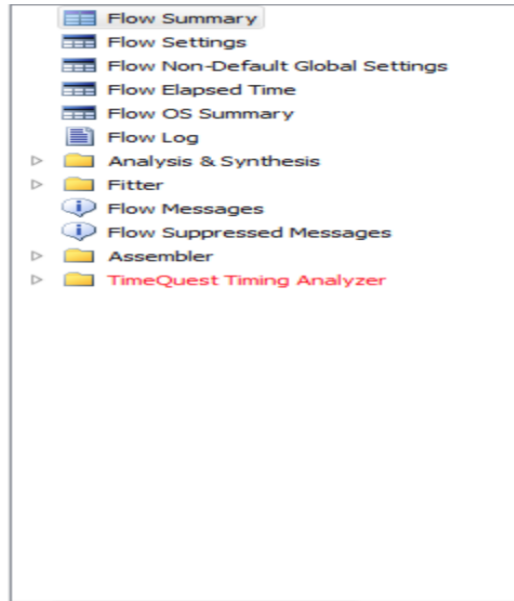



Figure 5.1: TimeQuest timing analyzer tab in the console

After compiling this time, the timing constraint report is red as shown in Figure 5.1, indicating that the timing is wrong, but generally for some small program mentioned before, it can be run. A red error indicating the negative slack will be reported at this time as shown in Figures 5.2 – 5.4 (more descriptions can be found under the pictures).

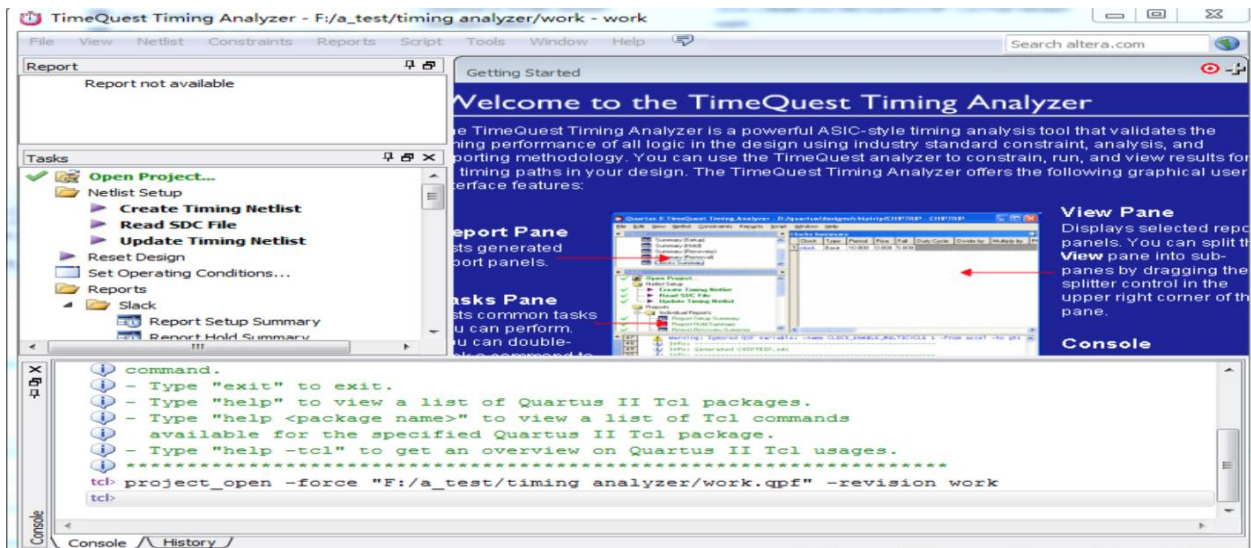


Figure 5.2: TimeQuest timing analyzer console

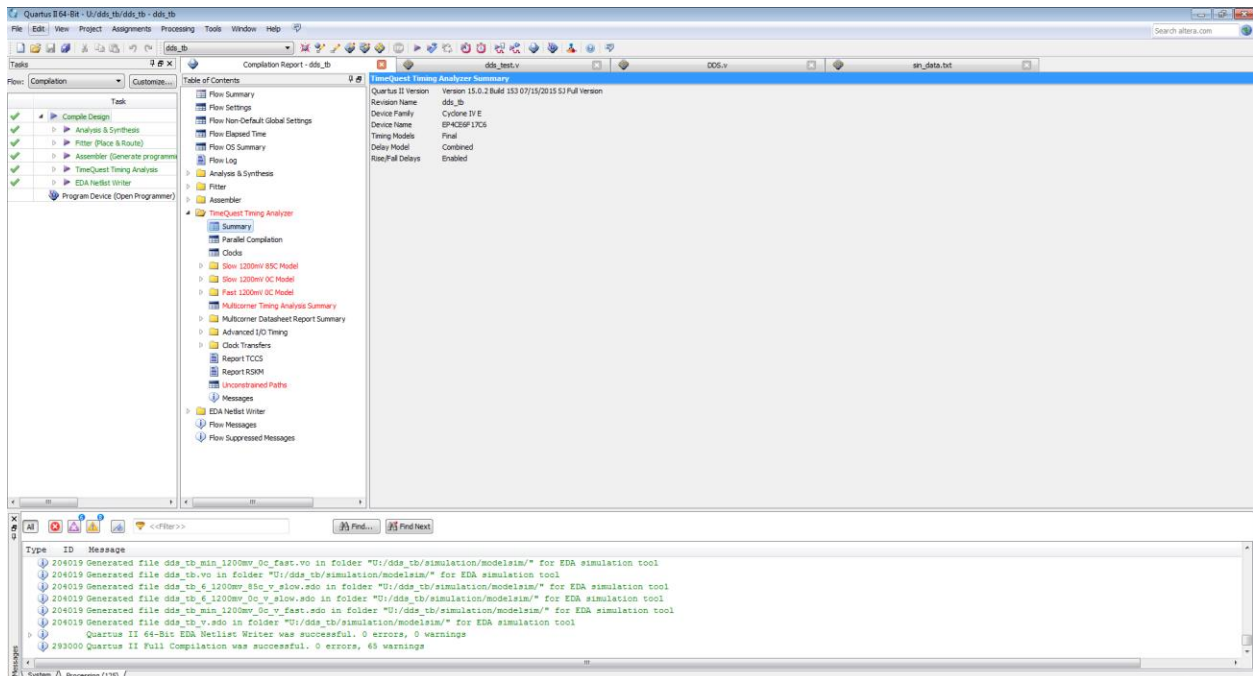


Figure 5.3: Compiling window showing successful compilation with timing not converged

Flow Log			
Analysis & Synthesis			
Fitter			
Assembler			
TimeQuest Timing Anal.			
Summary			
Parallel Compilati			
Clocks			
Slow 1200mV 85C Mo			
Fmax Summary			
Setup Summary			
Hold Summary			
Recovery Summar			
Removal Summary			
Minimum Pulse W			
Worst-Case Timi			
Datasheet Repor			
Metastability R			
Slow 1200mV OC Mod			
Fast 1200mV OC Mod			
Multicorner Timing			
Multicorner Datas			
Advanced I/O Timin			

	Clock	Slack	End Point TNS
1	CLOCK_50	-0.871	-4.300

Figure 5.4: Red error indicating the setup negative slack

The time at which the data of the input pin must appear before the clock is valid is called the setup time T_{su} ; the hold time T_h is the minimum time that the data must be held after the edge of the clock.

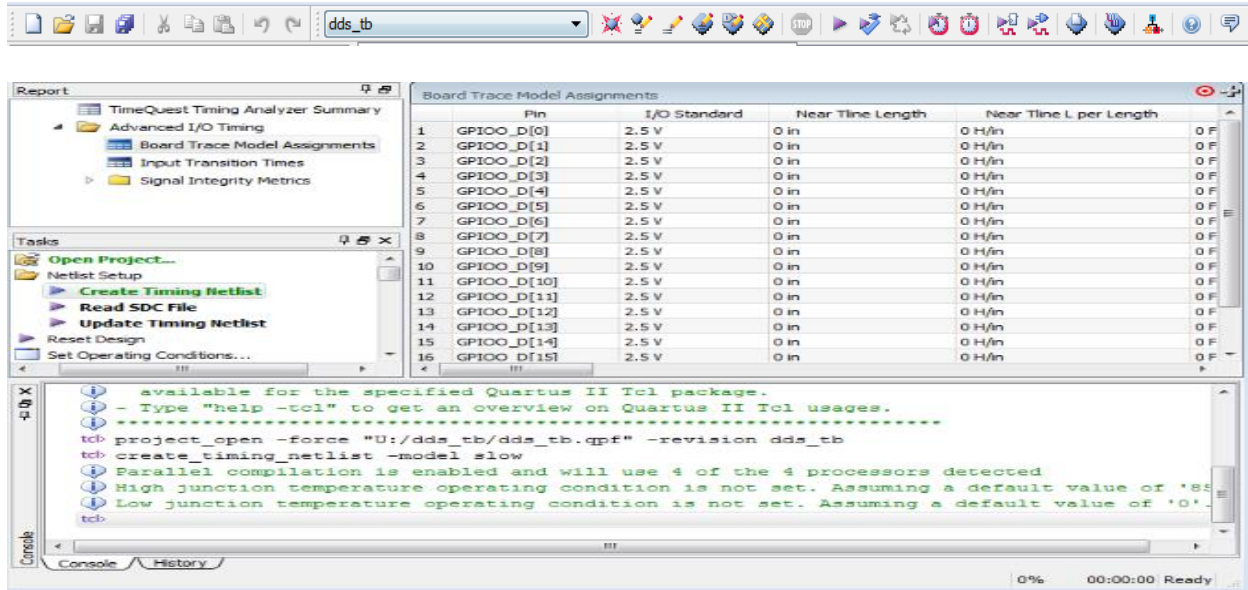


Figure 5.5: Console showing timing netlist generation successful

As shown in Figure 5.5, after the successful generation of Timing Netlist, the SDC file needs to be read in.

2). Include the Experiment code in .sdc file.

```
Create_clock -period 20.000 -name mainclk {get_ports {CLOCK_50}}}
```

```
Derive_pll_clocks
```

```
Derive_clock_uncertainty
```

3). Set a non-ideal clock.

The clocks we use are all non-ideal and generally give the clock a margin. Latency is the phase difference between the register clock signal and the clock source signal; the uncertainty is the phase difference of the clock signal between the register and the register, where the uncertainty is

set. Constraints->Set Clock Uncertainty sets the setup uncertainty of the clock source to 1 ns as shown in Figures 5.6–5.7 as procedures. When designing any circuit for an FPGA, the different processes involved will continuously try and optimize the code, thereby making it more efficient.

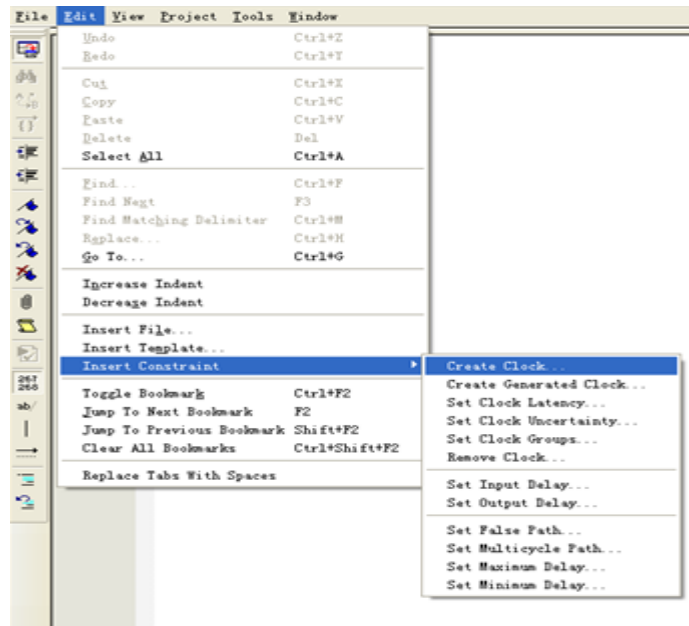


Figure 5.6: Create clock tab

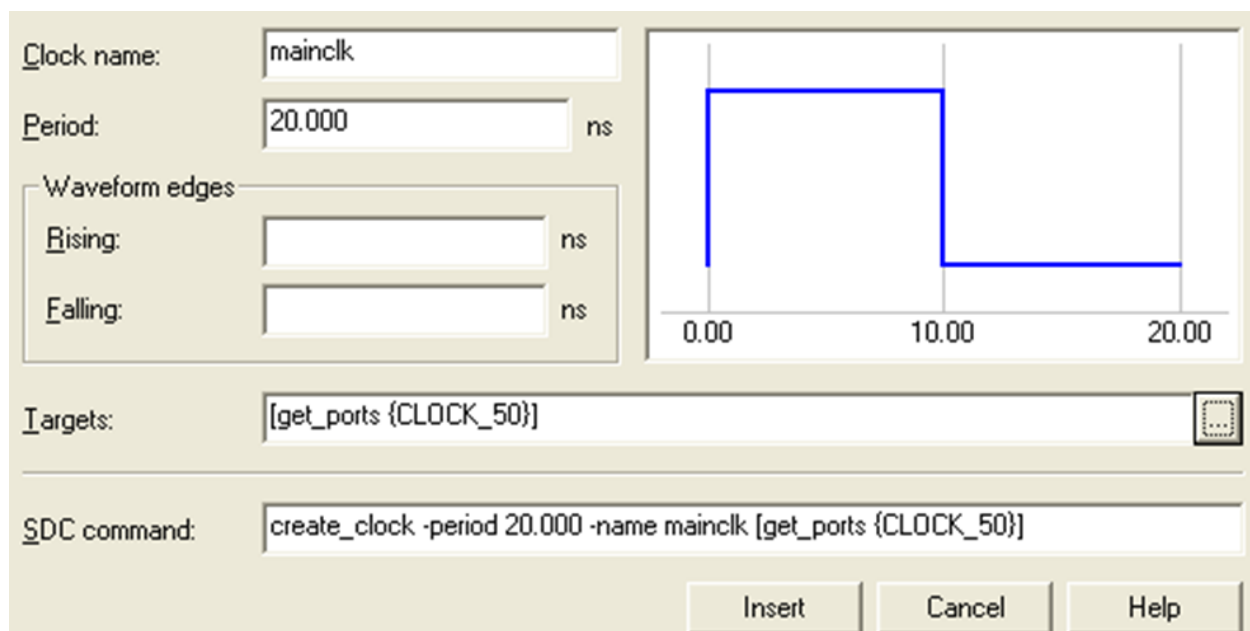


Figure 5.7: Create main clk with 50 MHz

```
Info: Report Timing: Found 10 setup paths (0 violated). Worst case slack is 17.815
```

Figure 5.8: Timing report

As shown in Figure 5.8, after recompiling, there is no more negative setup slack, which means there are no more setup timing violations in this design shown in the console. This chapter has discussed the final timing results and different simulation waveforms that were achieved with the DDS design for the FPGA.

CHAPTER 6: SPURS IN THE DDS

Due to the design's inherent qualities, the generated sinusoid is not perfect and contains certain disturbances/spikes/spurs. Following are the spurs the DDS's embedded spurs.

Phase Truncation Spurs: To design a smaller LUT which draws less power, we eliminate some of the least significant bits (LSBs) of the 32 bit word from the PA. This truncation of bits leads to spectral impurity known as phase truncation spurs, which are the biggest cause of noise and spikes in the DDS system. Since this part of the system is completely digitally designed, there are many algorithms that can be implemented to reduce these spurs.

Quantization Noise Spurs: In the DDS design presented here, we truncate the output of the LUT even further and then give it to the DAC. The DAC, however, accepts a signed binary number with a certain precision. To achieve this, the input bits are further rounded. This modification and quantization lead to quantization noise spurs.

Quantization Nonlinearity Spurs: According to the technical tutorial on DDS by Analog Devices, these spurs are caused by the inability to design a perfect DAC [2]. Due to the DAC's inherent design and non-ideal transfer function behavior, every input will have a few errors associated with it and thus one will not attain an ideal output. These errors, essentially caused by the non-linearity of the DAC, lead to quantization nonlinearity spurs that can only be reduced by increasing the precision of the DAC.

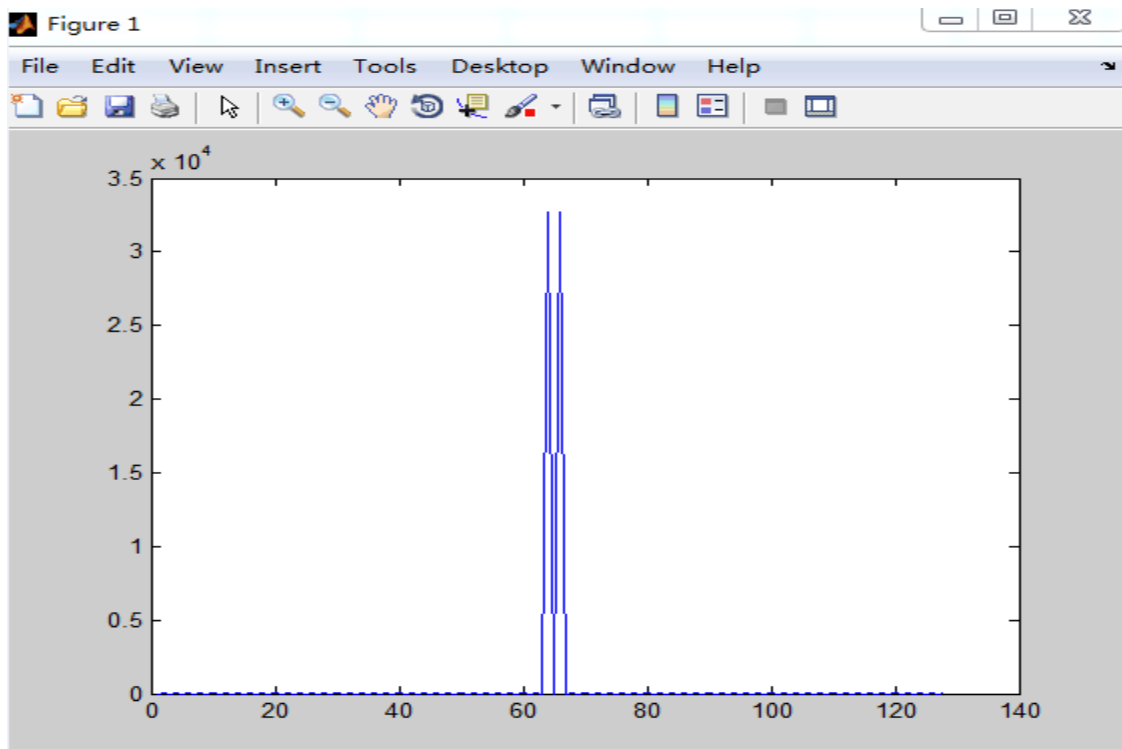


Figure 6.1: Phase truncation spur in traditional DDS

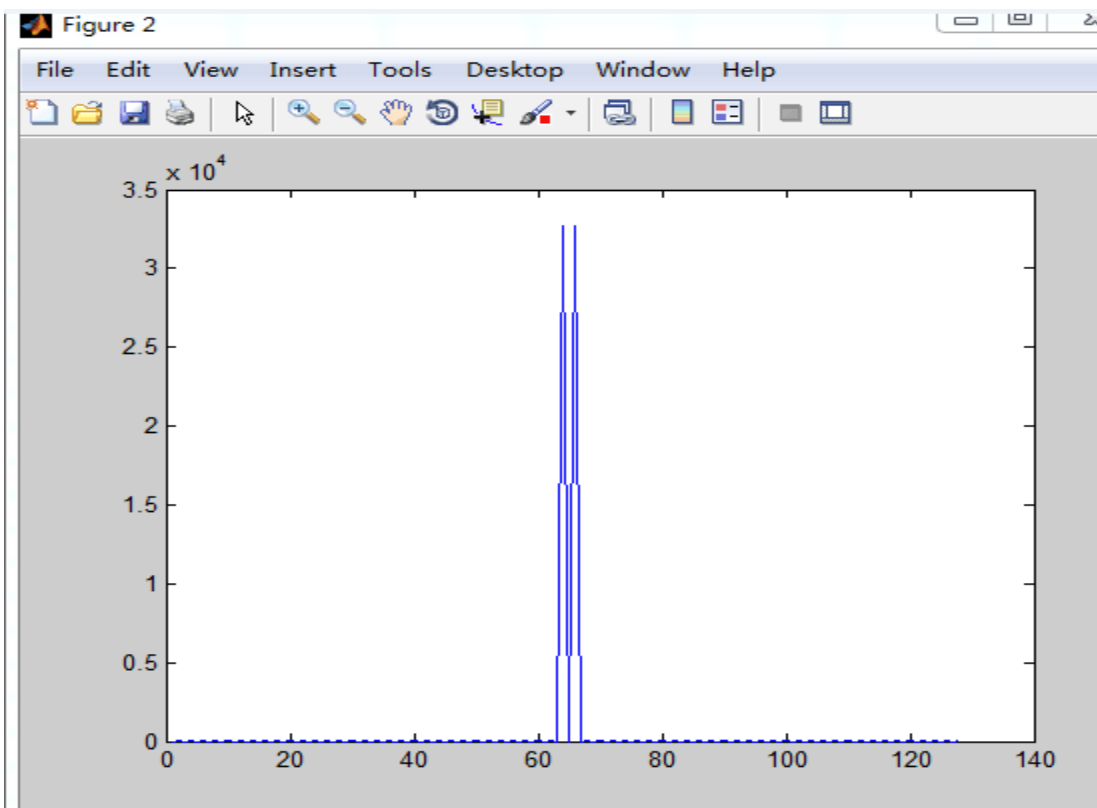


Figure 6.2: Phase truncation spur in new structure DDS

Based on Figure 6.1 and Figure 6.2, the phase truncation spur is almost the same for the traditional DDS and new structure DDS. There is not much difference in the spurious spur difference between the traditional DDS and new structure DDS, which is consistent with the goal: to minimize hardware complexity, reduce chip area and power consumption, and increase chip speed without sacrificing the signal quality of DDS.

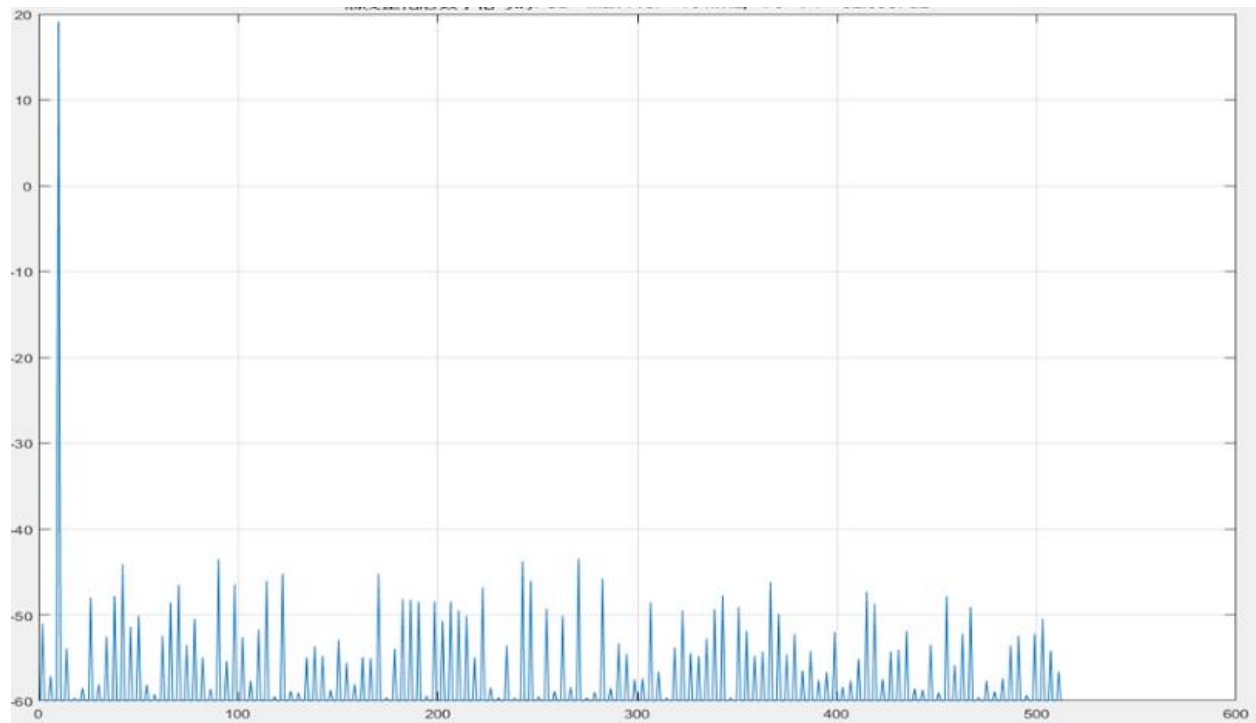


Figure 6.3: Power spectrum density result in Matlab

The Matlab simulation result of power spectrum density is shown above in Figure 6.3 with ($2^N=1024$).

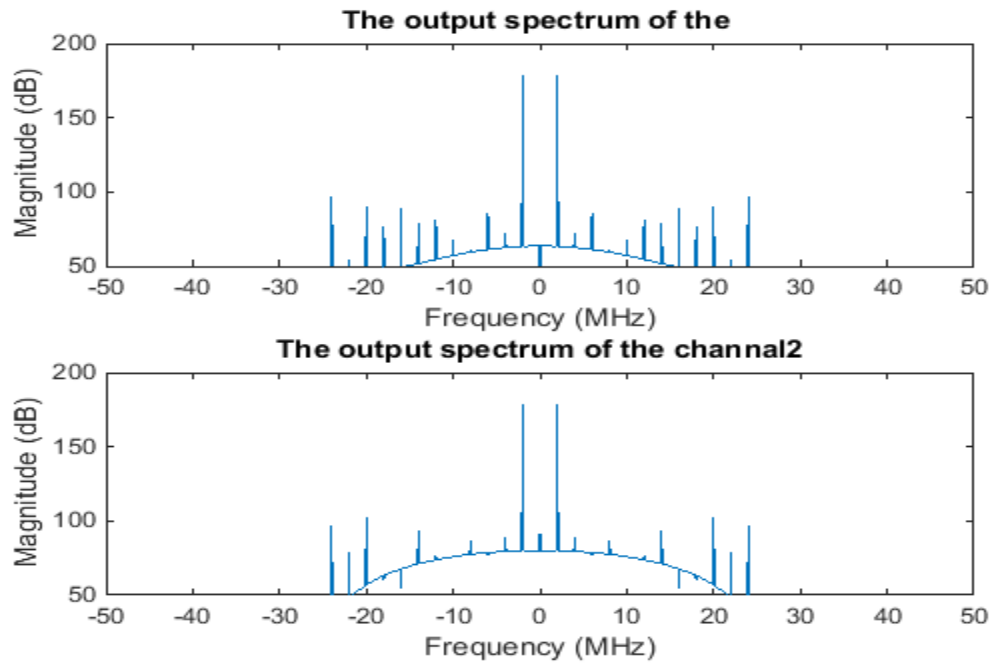


Figure 6.4: Output spectrum result in Matlab

Based on Figure 6.4, the harmonic frequency is much less than the output frequency: 178.34 dB at -2 MHz and 2 MHz. At -20MHz, the harmonic frequency is 102.12dB.

CHAPTER 7: CONCLUSION AND FUTURE WORK

In summary, this thesis laid down the path necessary to design any circuit for an FPGA, using a new structure of DDS as an example. The results for the new structure DDS were presented and they are consistent with the goal. Future research topics related to involving DDS in a more complex circuit design are also worth exploring. In the future, an ASIC approach to designing the DDS and fabricating the real circuit for testing is also worth exploring.

REFERENCES

- [1] T. M. Comberiate, “Phase noise spur reduction in an array of direct digital synthesizers,” M.S. thesis, University of Illinois at Urbana-Champaign, Urbana, IL, 2010.
- [2] Analog Devices, “A technical tutorial on digital signal synthesis,” Application Note, 1999.
Available: <https://www.analog.com/media/en/training-seminars/design-handbooks/Technical-Tutorial-DDS/technical-tutorial-DDS.pdf>
- [3] J. Tierney, C. Rader, and B. Gold, “A digital frequency synthesizer,” *IEEE Trans. Audio Electroacoust.*, vol. AU-19, no. 1, pp. 48–57, 1971.
- [4] D. A. Sunderland, R. A. Strauch, S. S. Wharfield, H. T. Peterson and C. R. Cole, “CMOS/SOS frequency synthesizer LSI circuit for spread spectrum communications,” in *IEEE Journal of Solid-State Circuits*, vol. 19, no. 4, pp. 497-506, Aug. 1984.
- [5] P. O’Leary and F. Maloberti, “A direct-digital synthesizer with improved spectral performance,” in *IEEE Transactions on Communications*, vol. 39, no. 7, pp. 1046-1048, July 1991.
- [6] S. Morteza pour and E. K. F. Lee, “Design of low-power ROM-less direct digital frequency synthesizer using nonlinear digital-to-analog converter,” in *IEEE Journal of Solid-State Circuits*, vol. 34, no. 10, pp. 1350-1359, Oct. 1999.
- [7] G. Chen, D. Wu, Z. Jin and X. Liu, “An ultra-high-speed direct digital synthesizer MMIC,” in International Conf. Millim. Wave Techn., Chengdu, China, 2010.
- [8] National Instruments, “Understanding direct digital synthesis,” Application Note, 2006.
Available: <http://www.ni.com/white-paper/5516/en/>

- [9] K. Bhagat, “Tutorial on designing and implementing a direct digital synthesizer (DDS) on a field programmable gate array (FPGA),” M.S. thesis, University of Illinois at Urbana-Champaign, Urbana, IL, 2012.
- [10] Y. Yang, J. Cai and J. Schutt-Aine, “A novel truncation spurs free structure of direct digital synthesizer,” *COMPEL - The International Journal for Computation and Mathematics in Electrical and Electronic Engineering*, vol. 32 issue no. 2, pp. 454 – 466, 2013
- [11] B. Mullane and C. MacNamee, “Developing a reusable IP platform within a system-on-chip design framework targeted towards an academic R&D environment,” Circuits and System Research Centre (CSRC), University of Limerick, Limerick, Ireland. Web page. Available: <http://www.design-reuse.com/articles/16039/developing-a-reusable-ip-platform-within-a-system-on-chip-design-framework-targeted-towards-an-academic-r-d-environment.html>
- [12] M. Chaitanya, “FPGA design flow,” Available: <http://digitaltagebuch.wordpress.com/2012/11/26/fpga-design-flow/>, 2012.
- [13] FPGA Design Flow Overview, FPGA Central, Available: <http://www.fpgacentral.com/docs/fpga-tutorial/fpga-design-flow-overview>, 2009.
- [14] Intel, “DE2-115 User Manual,” Available: <https://www.intel.com/content/www/us/en/programmable/solutions/partners/partner-profile/terasic-inc-/board/altera-de2-115-development-and-education-board.html?wapkw=de2-115+user+manual#overview>, 2018.
- [15] S. Li, “Tutorial on designing and simulating a truncation spurs-free direct digital synthesizer (DDS) on a field-programmable gate array (FPGA)” M.S. thesis, University of Illinois at Urbana-Champaign, Urbana, IL, 2015